Journal of Geomatics Vol 8 No. 2 October 2014

Fusion of ascending and descending pass high resolution SAR data

R. Chandrakanth[1], J. Saibaba[1], Geeta Varadan[1] and P. Ananth Raj[2]
[1]Advanced Data Processing Research Institute (ADRIN)
Dept. of Space, Hyderabad
[2]Dept. of Electronics and Communication Engg.
Osmania University, Hyderabad
Email: kanth_ravikanti@yahoo.co.in

(Received: Mar 25, 2014; in final form: Sep 17, 2014)

Abstract: It is well known that SAR images suffer from inherent layover, foreshortening and shadow effects apart from speckle noise. The fusion of ascending and descending pass SAR images overcoming these geometric effects. This paper presents a methodology for fusion of ascending and descending pass SAR images of high resolution. Due to difficulty in registration of ascending and descending pass SAR images owing to opposite viewing, the paper presents a methodology based on terrain correction followed by registration. While focusing on high resolution data the paper analyses the ascending and descending pass geometry of SAR images in selection of images for the success of fusion. The use of DEM based on SRTM and ASTER was analyzed with respect to the quality of terrain corrected product. Due to use of high resolution SAR data, a methodology for fusion of them based on saliency is proposed and presented. The results of registration and fusion are presented and analyzed. The proposed fusion technique was also applied on multipolarimetric SAR data and the results are presented.

Keywords: Image fusion, Ascending, Descending, SRTM, Layover, SAR, Registration, CFAR, Terrain correction

1. Introduction

Unlike EO (Electro Optical) imaging, SAR imaging by remote sensing satellites has unique advantage of acquiring images in both descending and ascending passes due to the presence of its own illumination source. In spite of all weather, day and night imaging capability, SAR imaging poses some pertinent limitations such as foreshortening, layover and shadow in hilly terrain due to side looking and range imaging nature of it. Hence, the fusion of ascending and descending pass images will have the advantage of overcoming some of these limitations. Also, it helps to obtain more complete information of point and distributed objects, both natural and manmade. Initially, such combinations were attempted for generation of DEMs by Radargrammetry (Leberl, 1989) methods particularly with ERS-1 and RADARSAT-1 images and later few attempts made towards fusion of them (Amarsaikhana, 2010; Guo, 2010; Sahyun Hong, 2002; Xinzheng Zhanga, 2007; Francis Canisius, 2004; Zhang, 2010). Unlike the popular fusion methodology like PAN sharpening, fusion of ascending and descending pass SAR images poses difficulties in registration and fusion due to opposite viewing geometry and scattering phenomenon. The fusion becomes even more difficult for high resolution SAR images of highly undulating terrains in the presence of built-up areas due to non availability of comparable resolution DEMs for terrain and 3D models for built-up features. However, the motivation for attempting fusion on these modes of images is due to presence and availability of high resolution SAR images with flexible acquisition configuration from multiple SAR missions like RISAT-1, TerraSAR-X – 1/2, RADARSAT – 1/2, COSMO SKYMED etc., and thereby better exploitation of SAR images. As the success of fusion lies in addressing registration and use of proper fusion technique, a registration methodology and fusion technique based on Neyman-Pearson criterion is proposed in this paper and their results are illustrated.

2. Data sets used

A typical layout depicting the ground coverage of ascending and descending passes of TerraSAR-X sample data (Astrium, 2013) described in table 1 is shown in Fig. 1. It shows the flight directions of ascending and descending passes along with their ground coverages.

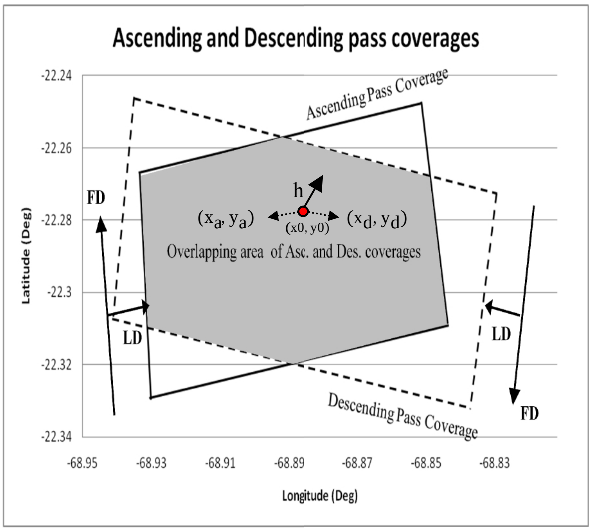

Figure 1: Ascending and descending pass coverage area and overlap region is shown in shaded area (FD – Flight Direction, LD – Look Direction)

Table. 1: Details of ascending and descending pass SAR images chosen for fusion

Details	**Ascending**	**Descending**
Date of Pass	26 Jan, 2009	30 Jan, 2009
Heading Angle	351°	186°
Look angle (mid swath)	35°	31°
Resolution	1m (az) / 1m (range)	1m (az)/ 1m (range)
Polarization	HH	HH
Look Direction	Right	Right
Imaging Mode	HS	HS

The images belong to the mine field of Chile. The depth of mine fields vary by as much as 600m over a span of 2500m approximately. Fig.1 illustrates ground displacements of an elevated feature at a height h above ground reference in ascending (x_a, y_a) and descending pass (x_d, y_d) images from its orthographic position (x_o, y_o). Conventional approaches for registration aims to align the images based on identification of GCPs and applying of suitable transformations $((x_d, y_d) \rightarrow (x_a, y_a))$. But due to opposite viewing geometry these displacements $((x_a, y_a),\ (x_d, y_d))$ will be large and varying depending on the complexity of topography. Though conventional approaches have reached automation to good extent (Suresh Kumar et al., 2012) but the identification of GCPs will become difficult even by robust similarity procedures like mutual information measure (Sahil and Peter, 2010) due to imaging of the same surface slope with different viewing mechanisms (layover, foreshortening and shadow) by ascending and descending passes and hence large variations in radiometry. In view of these factors an approach for registration is proposed. Also considering the dependency of foreshortening on look angles, selection of proper images is explained in the following section for the success of fusion.

3. Selection of data

In view o f the capability of present SAR missions to acquire images from extended low to extended high look angles (θ_l) as evident from RADARSAT-2, TerraSAR-X, RISAT-1 etc., suitable data can be selected for the success of fusion. Fig.2 depicts the typical acquisition geometries of ascending and descending passes. Due to range imaging elevated features in the SAR image get displaced (R_d) from its orthographic position according to

$$R_d = h \cot(\theta_l) \qquad (1)$$

where h is height of the feature above the reference ground plane as shown in Fig. 2.

It is known that layover and shadows occur according to:

i) Layover

$$\text{if } \theta_{ld} < \theta_{sf} \quad \text{----} \quad \text{Descending}$$
$$\theta_{la} < \theta_{sb} \quad \text{----} \quad \text{Ascending} \qquad (2)$$

ii) Shadow

$$\text{if } \theta_{ld} > \theta_{sb} \quad \text{----} \quad \text{Descending}$$
$$\theta_{la} > \theta_{sf} \quad \text{----} \quad \text{Ascending} \qquad (3)$$

where θ_{la} and θ_{ld} are look angles for ascending and descending passes respectively and θ_{sf} and θ_{sb} are surface front and back slopes respectively as shown in Fig. 2. Assuming symmetry in mountainous features i.e., $\theta_{sf} = \theta_{sb}$ and comparing eq. (2) and eq. (3) equal look angles will play an opposite role for front and back slopes for ascending and descending pass images. Further, since layover and shadow are complementary to each other as inferred from eq. (2) and eq. (3), either lower look angles or higher look angles can be used to meet the objective of fusion. In order to avoid foreshortening effects in the hilly regions and larger relief displacements due to built-up features particularly on high resolution images it is preferable to choose higher look angles for both ascending and descending passes (Leberl, 1989). But too large look angles will result in shadow dominance and hence fusion process needs to be focused on replacement of shadow regions rather than layover regions accordingly. From the point of better matching of high resolution features like roads on elevated features and to avoid radiometric mismatch due to foreshortening it is preferable to select ascending and descending pass images with near equal look angles. Also, selection of ascending and descending pass images with near equal look angles eases image registration in view of similar foreshortening effects.

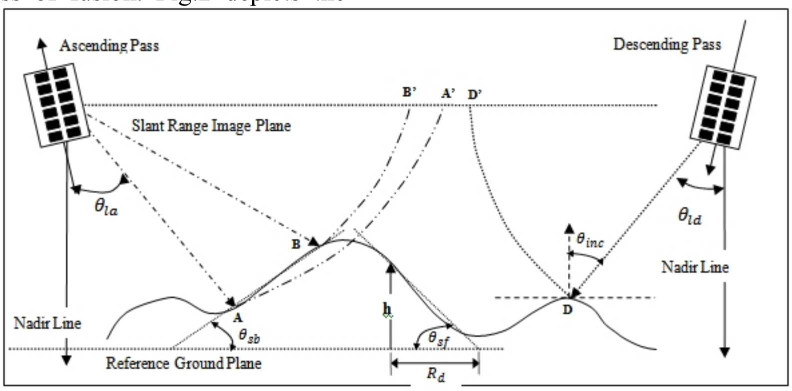

Figure 2: Acquisition geometry of ascending and descending pass SAR images

4. Registration

Conventional approaches for registration pose certain difficulties for ascending and descending pass SAR images of highly undulating surfaces due to 1) opposite relief displacements of elevated features, 2) precise identification of features and 3) different imaging conditions of facing and back slopes of a surface. Alternatively, orthorectification /Terrain Correction (TC) can be applied. The available geometric resolution and accuracy of SRTM and ASTER DEMs as well as that of SAR images are insufficient for achieving good registration, particularly for high resolution SAR images. Hence, a methodology based on combining orthortectification and GCP identification is proposed as shown in Fig. 3. Orthorectification corrects the relief displacements to the extent of resolution and accuracies of DEMs and SAR images. Hence, further registration is required by identification of GCPs preferably on plain regions followed by global / local transformations depending on the nature of inaccuracy of orthorectification results.

5. Fusion methodology

Since the objective of fusion of ascending and descending pass images is primarily to overcome layover and shadow effects in the undulating regions, accordingly a methodology is proposed as shown in Fig. 4. The plain region mask is also considered in the methodology for giving completeness to the point and distributed objects that are complementary in nature between ascending and descending images. The layover / shadow mask of either ascending / descending image only needs to be chosen since the fusion is inherently based on merging complementary information between them. In the plain regions selection of ascending and descending pixels is proposed based on saliency measure.

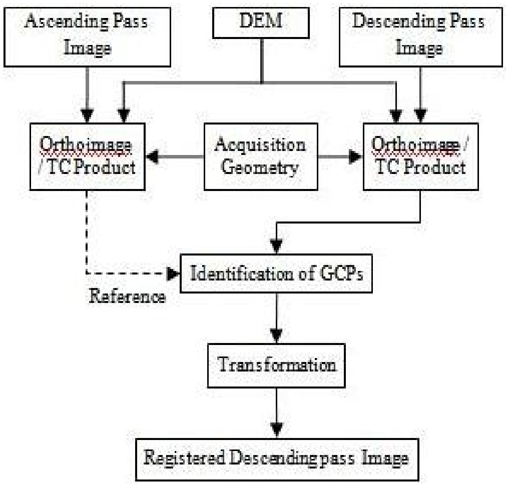

Figure 3: Flow diagram for registration of ascending and descending pass images

SAR being a coherent imaging system, the shapes of surface objects get manifested in the form of point targets with intensity variations rather than continuous shapes as in optical images. Also, the homogeneous surfaces get manifested in the form of constant intensity with speckle noise. In view of it a saliency measure ($\mathcal{S}$) to detect the objects is proposed based on two-parameter CFAR (Constant False Alarm Rate) (Oliver and Quegan, 1998) statistic given by:

$$\mathcal{S} = \frac{\frac{\mu_c}{\mu_b} - 1}{\sqrt{\nu_b}} \tag{4}$$

where, μ_c is intensity of central pixel and μ_b is mean of background surrounding it and ν_b is normalized variance of background. The background is considered as a ring of pixels surrounding the central pixel as shown in Fig. 5 to avoid influence of central pixel in the estimation of background statistics.

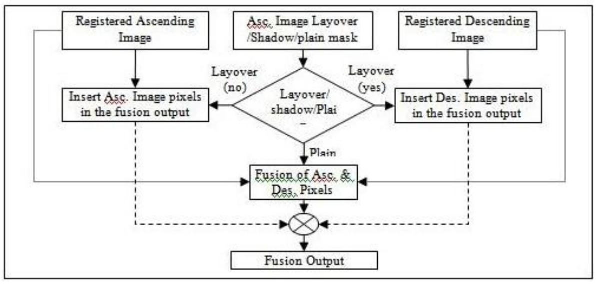

Figure 4: Flow diagram for fusion of ascending and descending pass SAR images

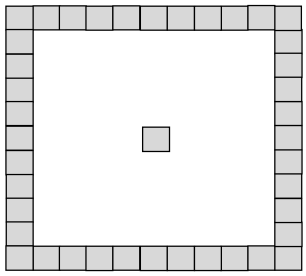

Figure 5: Illustration for computation of saliency

In the fusion, Neymann - Pearson criterion based on CFAR statistic (eq. 4) as given below can be used to decide whether a pixel is salient or not.

$$\frac{\frac{\mu_c}{\mu_b} - 1}{\sqrt{\nu_b}} > t \tag{5}$$

where t is a threshold that is based on allowable false alarm rate (P_{fa}). Assuming a constant background, P_{fa} is given by

$$P_{fa} = \frac{1}{\sigma_b}\int_t^{\infty} e^{-\frac{I}{\sigma_b}}\, dI \tag{6}$$

where, I is intensity and σ_b is Radar Cross Section (RCS) of background. Solving the above eq. (6) t can be related to P_{fa} as

$$t = -\sigma_b ln\, P_{fa} \tag{7}$$

The procedure for fusion in the plain region is summarized in the following steps:

Step 1: Select t based on assumed probability of false alarm P_{fa}.
Step 2: Compute μ_b and ν_b for a pixel under consideration.
Step3: Compute $\mathcal{S}$ based on eq.(4) for both ascending and descending pass images.
Step 4: If $\mathcal{S}$ is greater than mean of both the input pixels, then select the pixel with high saliency $\mathcal{S}$ for fusion output, otherwise consider mean of the pixels for fusion output.
Step 5: repeat steps 1 to 4 for all pixels in the plain region of the mask.

In the above fusion process, CFAR statistic (eq. 5) is used to detect whether central pixel under consideration is prominent or not based on threshold t, and the saliency measure of it (eq. 4) is used to find the most prominent response of the input images for fusion output. In absence of any prominent responses maximum likelihood estimate (mean) is considered for fusion output. Thus fusion output results in presence of low frequency details (homogeneous regions) with speckle noise reduction and appearance of most prominent responses among all input images. Thereby, it results in better completion and continuity of shapes by integrating information from all input images. Hence, the proposed procedure results in bringing complementary information as well as enhancement of supplementary information along with reduction of speckle in the homogenous regions in the fusion output.

6. Results and analysis

The images are orthorectified/terrain corrected by NEST software (Nest 2013). The orthorectified images are further registered by affine transformation. Fig. 6(c) and 6(d) show the result of orthorectification based on SRTM DEM. The corresponding original images of TerraSAR-X in their native acquisition geometry (range vs azimuth) are shown in Fig. 6(a) and 6(b) for ascending and descending passes respectively. Fig. 6(e) and 6(f) show the corresponding orthorectification result by use of ASTER DEM which is a product of METI and NASA (gdem 2013). The terrain predominantly consists of mining activity and is highly undulating in nature (800m variation from surface to deepest portion of minefield). It is to be noted that SRTM DEM is of 90m resolution and ASTER DEM is of 30m resolution. The comparison of results by use of both the DEMs shows the influence of resolution on orthorectification process. The spreading of layover region in descending and ascending passes is not complete in SRTM DEM orthorectification as compared with ASTER DEM (dotted circle).

Since the objective of fusion of ascending/descending pass images is to fill the layover / shadow regions present in one image with the other image, generation of layover / shadow mask is prerequisite for fusion. The layover / shadow and plain regions mask can be generated either from incidence angle map that can be obtained while generation of orthorectified image or directly from DEM by use of SAR acquisition geometry. Since ascending pass orthorectified image is used as reference image (Fig. 3) for registration, its incidence angle (θ_{inc} in Fig. 2) map image is used for generation of layover / shadow and plain region map. The theoretical criterion for layover/shadow and plain region mask is as follows:

$inc.angle = look\ angle$ ---- plain region
$inc.angle < look\ angle$ ---- Layover region
$inc.angle > look\ angle$ ---- Shadow region

For practical purposes, range of values around look angle can be considered. Fig. 7(a) depicts the layover/ shadow and plain region map that is generated by use of incidence angle map. Since the mask consists of erroneous regions, they need to be filtered for its use for fusion. Fig. 7(b) illustrates the mask after applying of morphological filters and area based filters based on connected component labeling (Jain, 1989) to remove islands within the large layover / shadow / plain regions.

The result of the proposed methodology for fusion of ascending and descending pass images shown in table-1 is illustrated in Fig. 8(a). The threshold t for CFAR detection is taken as 0.005. It is to be noted that threshold t controls preservation of point targets in the fusion output. The result of fusion in layover regions shown in

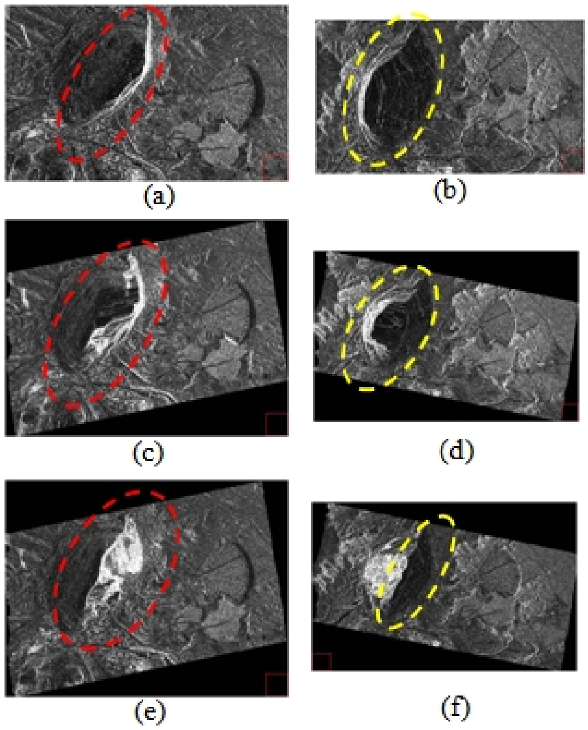

Figure 6: Result of orthorectification of ascending and descending pass images - Original images of (a) Ascending pass (b) Descending pass, Orthorectification using SRTM DEM of (c) ascending pass (d) descending pass, Orthorectification using ASTER DEM of (e) ascending pass (f) descending pass images

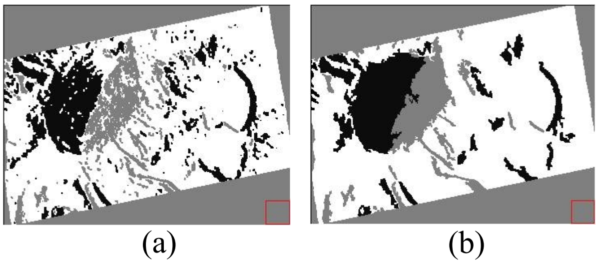

Figure 7: Generation of layover/shadow and plain region mask. (a) Mask generated by use of incidence angles and look angle of SAR (b) Mask after applying of morphological filters

Fig. 8(b) illustrates the quality of registration by the proposed methodology and advantage of fusion in overcoming the geometric distortions of SAR. It illustrates the continuity of features achieved by fusion of ascending and descending pass images. It also shows the advantage of selecting images of near equal look angles in bringing consistency of features of high resolution images. Fig. 9(c) shows the portion of the fused image in plain regions by the saliency based approach. Fig. 9(a) and 9(b) show the corresponding registered ascending and descending pass images. It clearly illustrates the advantage of fusion in combining complementary features in the formation of complete shapes of objects by the proposed method. The intersect region between ascending and descending shown in the Fig. 8(a) is due to presence of layover in both the ascending and descending regions. It also suggests that choosing of look angles greater than 35^o for this set of images would probably alleviate this common layover region.

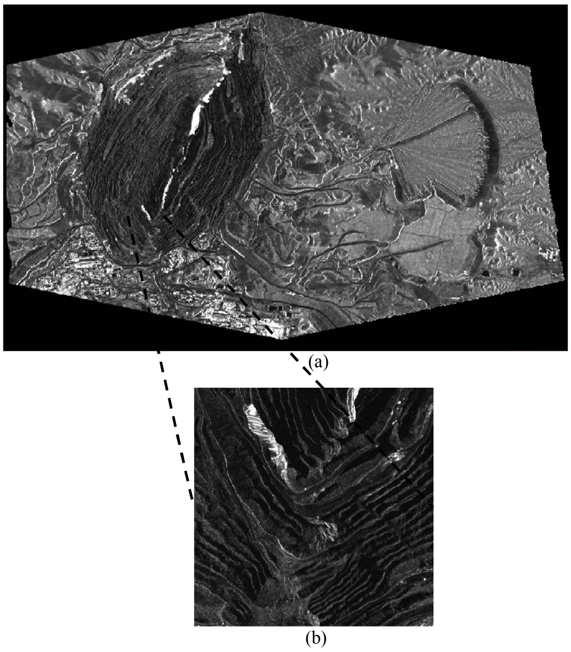

Figure 8: Result of fusion of Ascending and Descending pass images - (a) Fusion output by proposed method (b) Depiction of continuity of features by fusion of layover free portions from ascending and descending images

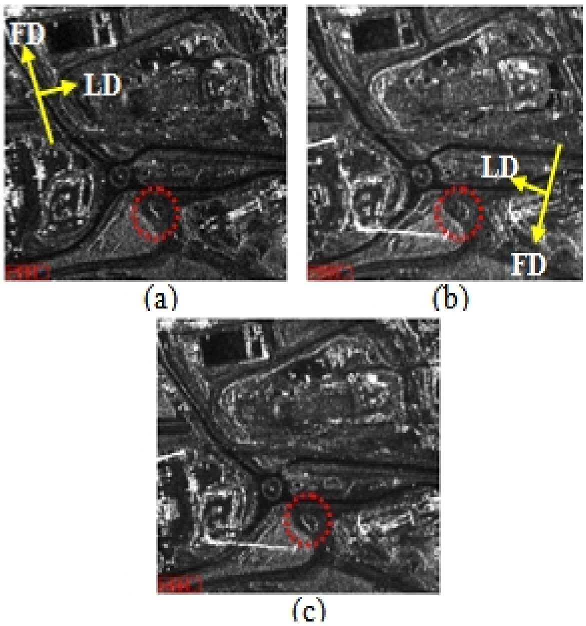

Figure 9: Results of fusion of ascending and descending pass SAR images (FD – Flight Direction, LD – Look Direction): Original Registered images of (a) Ascending pass, (b) Descending Pass; (c) merged by proposed method

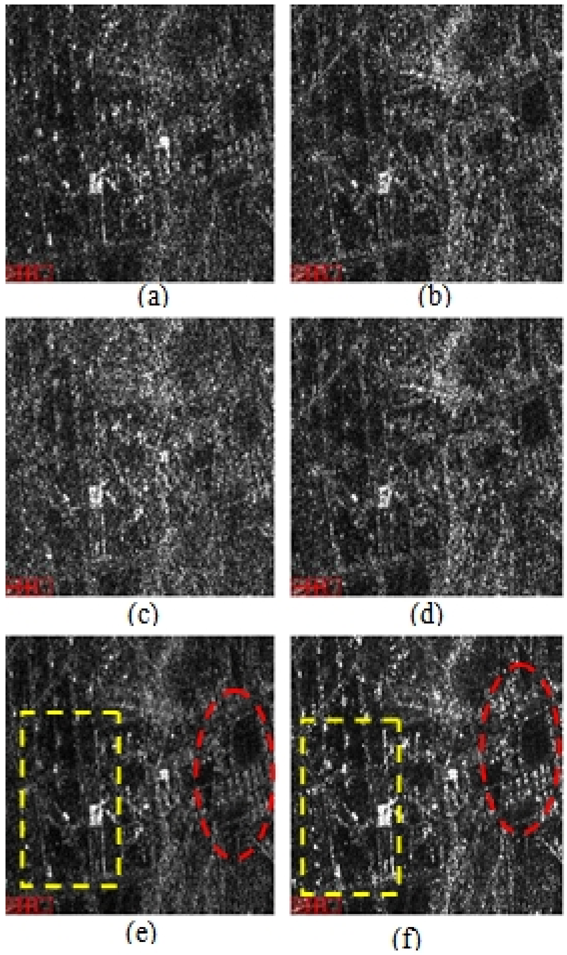

Figure 10: Results of multipolarization fusion. Original images of (a) HH, (b) HV, (c) VV and (d) VH polarization images. Fusion output by (e) Maximum likelihood (f) Proposed approaches

Table 2: Performance of multipolarization fusion

Image	Entropy	ENL	Overall Performance
HH	9.68	2.02	19.55
VV	9.58	1.86	17.81
VH	8.7	1.77	15.39
HV	8.7	1.77	15.39
Maximum Likelihood	9.24	3.00	27.72
Proposed Method	9.29	3.08	28.61

Fig. 10 illustrates the saliency based fusion applied on polarimetric images RADARSAT-2. Fig. 10(a) to 10(d) show the quad polarization images used for fusion. The result of fusion by the proposed method is shown in Fig. 10(f). Fig. 10(e) shows the result of fusion by maximum likelihood. The results are evaluated based on entropy and effective number of looks (ENL). Table 2 lists the evaluation results. Though entropy for HH and VV is higher than fusion output but it is not an indicative of true information due to presence of higher speckle noise as shown in the ENL column in the table. Hence, combined performance is shown by multiplying entropy and ENL in the overall performance column. The overall performance clearly indicates the advantage of fusion by proposed methodology.

7. Conclusions

The advantage of fusion of ascending and descending pass images of high resolution SAR data over undulating terrain was presented. Due to opposite viewing, importance of selection of data was critically analysed. Registration methodology based on terrain correction and identification of GCPs was proposed. The results of terrain correction based on SRTM and ASTER DEM are compared. A hybrid methodology for fusion based on layover / shadow / plain region mask and saliency measures are proposed and illustrated and evaluated. Finally, it is suggestive to develop registration methods based on matching of object features with the help of DEMs that will greatly help in registration to a sub-pixel level particularly for built-up areas.

Acknowledgments

The authors are extremely thankful to Sri S K Patra and Sri P Suresh Kumar for their valuable suggestions.

References

Amarsaikhana, D., H.H. Blotevogelb, J.L. van Genderenc, M. Ganzoriga, R. Gantuyaa and B. Nerguia (2010). Fusing high-resolution SAR and optical imagery for improved urban land cover study and classification, International Journal of Image and Data Fusion, vol.1, no.1, pp. 83 - 97.

Francis Canisius, et al., (2004). Fusion of Ascending and Descending Pass SAR Intensity and Coherence Images for Mapping Volcanic Deposits, Geocarto International, vol 19, issue 3, pp. 43 – 50.

Guo, R., L. Zhang, M. Xing and J. Li (2010). Polarimetric SAR image fusion using nonnegative matrix factorisation and improved-RGB model, Electronics Letters, vol. 46, no. 20, pp. 1399-1401.

Jain, A.K. (1989). Fundamentals of digital image processing. Prentice Hall.

Leberl, F.W. (1989). Radargrammetric image processing, Artech House Inc.: Massachusetts.

Oliver, C. and S. Quegan (1998). Understanding synthetic aperture radar images. Artech House, Boston.

Sahil, S. and R. Peter (2010). Mutual information based registration of Terrasar-X and IKONOS imagery in urban areas, IEEE Trans. Geosci. Remote Sens., vol. 48, pp. 939–949.

Sahyun Hong, W M. Moon, Hong-Yul Paik, Gi-Hyuk Choi (2002). Data Fusion of multiple Polarimetric SAR images using Discrete Wavelet Transform (DWT), IGARSS-02, vol.6, pp.3323-3325.

Suresh kumar, P., R. Chandrakanth, N. Mishra, J. Saibaba and G. Varadan (2012). A generalized search scheme for automatic registration of remote-sensing data, Int. J. of Remote Sensing, vol.33, no. 2, pp.490-501.

Xinzheng Zhanga, Peikang Huangb, Ping Zhoua (2007). Data fusion of multiple Polarimetric SAR images based on combined curvelet and wavelet transform, APSAR-07, pp.225-228.

Zhang, J., J. Wei, G. Huang and H. Zhang (2010). Fusion of ascending and descending polarimetric sar data for colour orthophoto generation, ISPRS TC VII Symposium – 100 Years ISPRS, Vienna, Austria.
http://www.astrium-geo.com/en/23-sample-imagery, 2013.

http://nest.array.ca/web/nest, 2013.

http://gdem.ersdac.jspacesystems.or.jp, 2013.